JOURNAL OF THE BALKAN GEOPHYSICAL SOCIETY, Vol. 2, No 4, November 1999, p. 139-150, 9 figs.

Determination of crustal and upper mantle structure between Iran and Turkey from the dispersion of Rayleigh waves

Altan Necioglu

Ankara Universitesi, Fen Fakultesi, Jeofizik Muh. B., Tandogan, 06100 Ankara, Turkey.
E-mail: necioglu@science.ankara.edu.tr

(Received 21 April 1998; accepted 9 September 1998)

Abstract *: To determine the crustal and upper mantle structure between Iran and Turkey, Rayleigh wave portions of the vertical component SRO-ANTO (**S**eismic **R**esearch **O**bservatories- **AN**kara **T**urkey **O**bservatory) records of eight earthquakes from Iran and one from eastern Turkey were analysed. One Station Method was used to calculate Rayleigh wave phase velocities in the period range of 12 to 48 seconds.*

Theoretical phase velocities for different earth models were computed and comparisons of the calculated and theoretical phase velocities were made. Perturbations of the model parameters were carried out until the best fit was obtained. Six acceptable models with 4 crustal layers (the first 2 may be sedimentary) were found. The average crustal thickness has been estimated to be between 52 and 56 km along the path from eastern Iran to ANTO, between 45 and 48 km along the path from western Iran to ANTO and between 42 and 44 km along the path from eastern Turkey and northwestern Iran to ANTO. The total thickness of the crust decreases by 14 km from Iran to ANTO in east-west direction.

Key Words: *Crustal Structure, Rayleigh Waves, Dispersion.*

INTRODUCTION

The seismic waves generated by an earthquake and recorded by a seismograph are controlled by; 1) mechanisms at the focus, 2) properties of the medium, and 3) response characteristics of the seismograph. Only the characteristics of the seismograph are known. The other two factors are not known beforehand and have been the subjects of investigations by seismologists.

The investigations of the properties of the medium are carried out by utilising the body waves and surface waves. Body wave travel times especially those of P phases provide valuable information.

Akaschek and Nassari(1972), estimated the crustal thickness to be 56±6 km for the central and western regions and 54±6 km for the northern region of Iranian plateau and the corresponding P wave velocities to be 8.13 ± 0.07 km/s for the western and 8.19 ± 0.06 km/s for the northern region from the travel times of P_n phase. Eslami (1974) estimated the crustal thickness of Shiraz area to be 42 ± 7 km by using the travel time curves of P waves from the earthquakes having the hypocentres below the crust. Chen *et al*. (1980) estimated the crustal thickness to be 49 km in the southern part and 34 km in the northern part of Iran and a uniform, poorly determined crust of 30 km thickness for Turkey by using upper mantle P wave velocity from the travel times. Asudeh (1982a), applied Two-Station method on the earthquake data in Iran to obtain P_n velocities along several paths between seismograph station pairs on the same great circle and estimated average P_n velocities to be 8.30 km/s for Zagros, 7.85 km/s for eastern Iran, 7.9 km/s for northwestern Iran and 8.2 km/s for central Iran. In another publication, Asudeh (1982b) calculated the phase velocities of fundamental mode Rayleigh waves between stations in Iran. For the Iranian plateau, an Alpine type crust was obtained whereas upper-most mantle velocities ranged from low-velocity mantle in eastern Iran to high velocity shield-like structure in western Iran. The crustal thickness was estimated to be 43, 45 and 46 km for eastern, central and western-southwestern Iran, respectively. Sneyder and Barazangi (1986) used data of 9000 gravity measurements to infer deeper crustal

structure under Zagros mountain-belt. They estimated Moho dips about 1^0 toward northeast beneath the folded belt. The dip increases to 5^0 near main Zagros thrust. The depth of Moho increases from 40 km under Arabian Gulf to 65 km under the thrust. Necioglu *et al.* (1981) estimated the crustal thickness of northwestern Turkey to be 28 ± 3.45 km using P wave travel times from the data of 43 Turkish earthquakes recorded by 14 Turkish seismograph stations.

The dispersion properties of surface waves have widely been used to determine the Earth's structure. Canitez and Ezen(1975) in an attempt to obtain crustal and upper mantle structures analysed the surface waves from two Turkish earthquakes recorded at European, Asian and African seismograph stations and they estimated that the crustal thickness ranges between 37 and 45 km in the region of their interest.

The dispersion properties of Rayleigh waves were utilized in this study to investigate the earth's structure between the earthquake foci and the recording station ANTO for 9 earthquakes occurred in eastern and western Iran and in eastern Turkey. In the period range of 12 to 48 seconds the Rayleigh wave phase velocities were computed using One Station Method of Brune *et al.* (1960). Herrmann's (1978) computer program was used to obtain the theoretical phase velocities from the earth models.

METHODS FOR THE PHASE VELOCITY DETERMINATION

Dispersion of a wave means that the wave velocity is the function of its frequency. This phenomenon has been observed in surface wave propagation and utilised in the investigations of the Earth's interior. It is closely related to the elastic parameters and the geometry of the layered medium.

Theoretically Rayleigh waves in a homogeneous medium do not show dispersion. But, the Rayleigh waves observed in seismology are dispersive because of the heterogeneity of the medium that waves pass through. The dependence of the phase velocity on the frequency is specified by a relation known as the dispersion equation of the form $g(c,w) = 0$.

Consider a time-harmonic wave, excited at $x = 0$, of the form;

$$u(x,t) = A(\omega) \exp i[\omega t - k(\omega)x], \qquad k(\omega) = \omega/c(\omega) \quad (1)$$

where the phase velocity is some function of frequency. If $u(0,t) = F(t)$, a transient, the solution will be superposition of harmonic components in the form of the integral;

$$u(x,t) = 2\,\mathrm{Re}\int_0^\infty A(\omega) \exp\{i\omega[t - x/c(\omega)]\}d\omega \quad (2)$$

which may also be written as

$$u(x,t) = 2\int_0^\infty A(\omega)\cos[x\, f(\omega) + \phi(\omega)]\, d\omega \quad (3)$$

$$f(\omega) = \omega\, t/x - k(\omega)$$

The group velocity, $U = U(w)$, is defined as the velocity with which a narrow band of frequency components within the wave form propagates. If a narrow band of frequencies $\Delta\omega$, is centred about the specific frequency w_o, the contribution of this band to the total signal at some point x, is then given by

$$u_{\Delta\omega}(x,t) = 2\,\mathrm{Re}\int_{\omega 0-\Delta\omega/2}^{\omega 0+\Delta\omega/2} A(\omega)\exp\{i[\omega t - k(\omega)\, x + \phi(\omega)]\}d\omega \quad (4)$$

If the exponent is expanded into a Taylor series about ω_0, the following expression is obtained:

$$[\dot{u}_0 t - k(\dot{u}_0)x + \phi(\dot{u}_0)] + [t - \frac{dk(\dot{u}_0)}{d\dot{u}}x + \frac{d\phi(\omega_0)}{d\dot{u}}](\dot{u} - \dot{u}_0)... \quad (5)$$

where the higher order terms are neglected, since $(\omega-\omega_0)$ is small. Equation (4) becomes

$$u_{\Delta\omega}(x,t) = 2\,\mathrm{Re}\, A(\omega_0)\exp i[\omega_0 t - k(\omega_0)x + \phi(\omega_0)] + \int_{\omega_0-\Delta\omega/2}^{\omega_0+\Delta\omega/2}\{\exp i[t - dk(\omega_0)/d\omega.\, x + d\phi(\omega_0)/d\omega](\omega - \omega_0)\}d\omega \quad (6)$$

The integral evaluated is of the form; $sin(X/X)$ where X is equal to

$$X = [t - dk(\omega_0)/d\omega\,.\,x + d\phi(\omega_0)/d\omega]\,\Delta\omega/2$$

The displacement may then be written in the form

$$u_{\Delta\omega}(x,t) = 2\,A(\omega_0)\cos[\omega_0 t - k(\omega_0)\, x + \phi(\omega_0)][(\sin X)/X] \quad (7)$$

From this equation it can be seen that the wave motion is a cosine function which is being modulated by a $sin(X)/X$ function. The interesting phenomenon is that the two propagate with different velocities. The cosine function propagates with a phase velocity of $U(w_0)$.

Since the highest amplitude occurs at X=0, the main contribution to the total energy at a fixed x and t is subject to the condition;

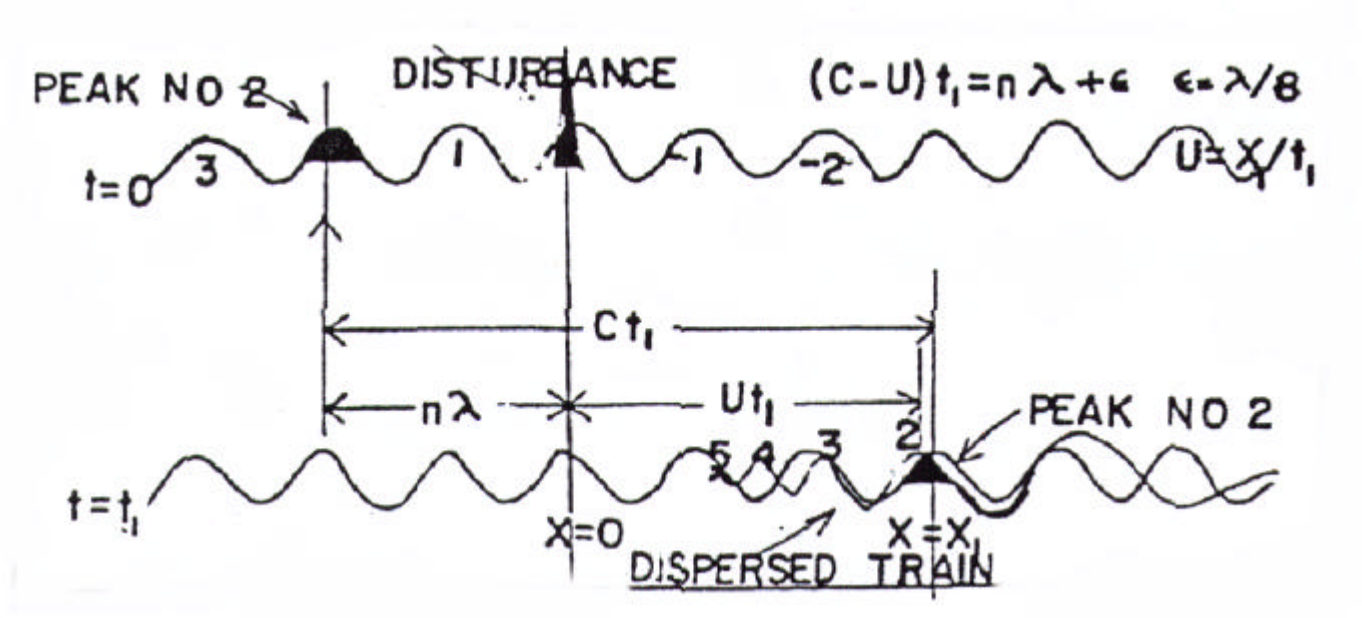

FIG. 1. Diagram indicating the conventions established for numbering peaks and illustrating the physical significance of phase velocity equation.

$t = (dk/d\omega)x - d\phi/d\omega$, $dt = (dk/d(\omega))\, dx$

Then the group velocity is written as

$$U(\omega_0) = dx/dt = d\omega/dk = c(\omega_0) - \lambda\, dc(\omega_0)/d\lambda \qquad (8)$$

where λ is the wavelength.

Knowing the distance *x* and travel time *t*, one can deduce group velocities as a function of phase velocities. The graph of the group velocity versus period is a tool that may be used for interpretation of lithospheric structure. The key to the use of surface waves for interpretation lies in the fact that the depth to which a wave penetrates is a function of its wavelength. Long period waves penetrate deeper. Thus the longer period waves arrive first, since they travel with a greater velocity. It follows that the dispersion curves should reflect the differences in the distribution of physical properties along the path.

Phase and group velocity curves may be obtained by plotting the velocities for a number of periods. Interpretation of this in terms of crustal structure is then possible by calculating what the group or phase velocity curve would be for specific models of crustal structure. The variables in such models are layer thickness, density and elastic moduli.

Experimental determination of phase velocities described in the equation (8) is called Two-Station Method. In this method, the records at two recording stations falling in the same great circle path are used to calculate the phase velocity using the equation:

$$C(T) = \frac{\Delta_b - \Delta_a}{t_b - t_a} \qquad (9)$$

where; Δ_b and Δ_a are the epicentral distances of two stations *b* and *a*, respectively. t_b and t_a denote arrival times to stations *b* and *a* and T is the period of the total wave motion. *n* denotes the peak number of total motion

This method eliminates the need for the knowledge of the initial phase. However, in the region of interest there were no stations located on the great circle path between the epicentres and ANTO. Therefore, One Station Method was utilised.

According to this method, a disturbance at one point of a dispersive medium resulting from an impulse applied at another point may be represented as a superposition of travelling plane waves. All attention is fixed on the peaks of the waves and various peaks are identified by numbering them according to their distance from the origin at the time of initiation of disturbance as shown in Figure 1. A peak of 35 wavelengths behind the origin at *t*'=0 will be assigned the order number 3.5 and so on. A peak in front of the origin at *t*=0 will be given a negative number. In general at *t*=0, a peak of travelling wave frequency w_0 will be located $N - (f_0/2p)$ wavelengths behind phase of the wave. The quantity $N-(f_0/2p)$ is defined as the order number, n, of the peak. After a travel time t, the peak will arrive at a distance x from the origin. Considering Figure 1 and applying elementary principles we may immediately write the equation for the motion of the peak as follows:

$$Ct - x = [N - (\phi_0/2\pi)] = n\lambda = [N - (\phi_0/2\pi)]CT \qquad (10)$$

where λ is the wavelength. In this equation, *t* corresponds to the travel time of a peak of one of the component travelling waves. In general, this may not correspond to the time t_1 of arrival of a peak of the total motion of the record since the total motion is determined by the superposition of infinite number of such travelling waves.

A peak of dispersed motion with frequency w_o, occurs when the peaks of the travelling wave components with frequencies equal and near w_o constructively interfere with one another, but the phase of the total motion will be *p/4* or *T/8* (where *T* is a period of the wave) different from the phase of the component travelling wave of the same frequency. An additional *-T/8* phase shift will be introduced for propagating cylindrical waves. The frequency of the total motion is determined by the customary method of measuring the slope of a plot of the peak number versus arrival time. The arrival time of the component of the travelling wave of this frequency is determined by adding or subtracting *T/8* seconds from the arrival time of the peak of the total motion. For normal branches of dispersion (*dU/dt>0*) correction is subtracted from the arrival time and for inverse dispersion (*dU/dt<0*) the correction is added. Here *U* is the group velocity defined as x_1/t_1 (Brune *et al.*, 1960).

Starting from above explanation the phase velocity can be given by the formula:

$$C = \frac{x}{t - \{[\phi_b - \phi_0]/2\pi + N - 1/8 \pm 1/8\}T} = \frac{x}{t - [n - 1/8 \pm 1/8]T} \qquad (11)$$

where x is the distance between source and station. ϕ_0 is the initial phase of the wave component, assumed to be independent of frequency. ϕ_b is the phase observed on the record. *N* denotes the numbers assigned successively to the phases (crest and trough), *t* is the travel time and *T* is the period.

If only peaks and troughs on the record are considered, then ϕ_b is either 0 or π and *N* are successive integers. In this work $\phi_b = 0$ for both crests and troughs but then *N* must be an integer for crests and an integer plus 0.5 for troughs. Therefore, the formula for the phase velocity calculations becomes;

$$C = \frac{x}{t - [N - \phi_0/2\pi = m]T} = \frac{x}{t - [n + m]T} \qquad (12)$$

where $m = -1/8 \pm 1/8$ and $n = N - (f_0/2p)$. Reasonable initial phase ϕ_0 can be equal to 0, $\pi/4$ or $\pi/2$. It can be seen that by assigning discrete sets of values, the phase velocity can be obtained. The main difficulty in applying the One Station Method is to distinguish which set is the closest to the real set of phase velocities.

To apply this method the waves must be well dispersed and amplitudes must not vary too rapidly

Table 1. List of the earthquakes studied.

EVENT #	REGION	DATE	ORIG.TIME	GEOGRAPHICAL COORD.	DEPTH	MAGN	EPI.DIST
1	IRAN	04.11.1978	15:22:20	37.614 N 48.836 E	33 KM	6.0	1415.3
2	IRAN	28.03.1979	01:33:28	30.969 N 50.046 E	33	5.0	1847.0
3	IRAN	30.09.1979	20:42:37	28.014 N 54.785 E	33	4.6	2408.7
4	IRAN	15.11.1079	05:06:55	34.013 N 59.937 E	33	4.5	2493.3
5	IRAN	23.11.1979	18:22:45	34.087 N 59.906 E	10	4.9	2487.5
6	IRAN	27.11.1979	17:12:34	33.903 N 59.800 E	10	5.0	24.86.5
7	IRAN	09.12.1979	09:12:00	35.033 N 56.811 E	33	5.1	2184
8	IRAN	16.12.1979	22:35:39	33.781 N 59.257 E	33	5.0	2445.9
9	E.TURKEY	11.04.1979	12:14:26	39.000 N 43.972 E	33	4.9	966.8

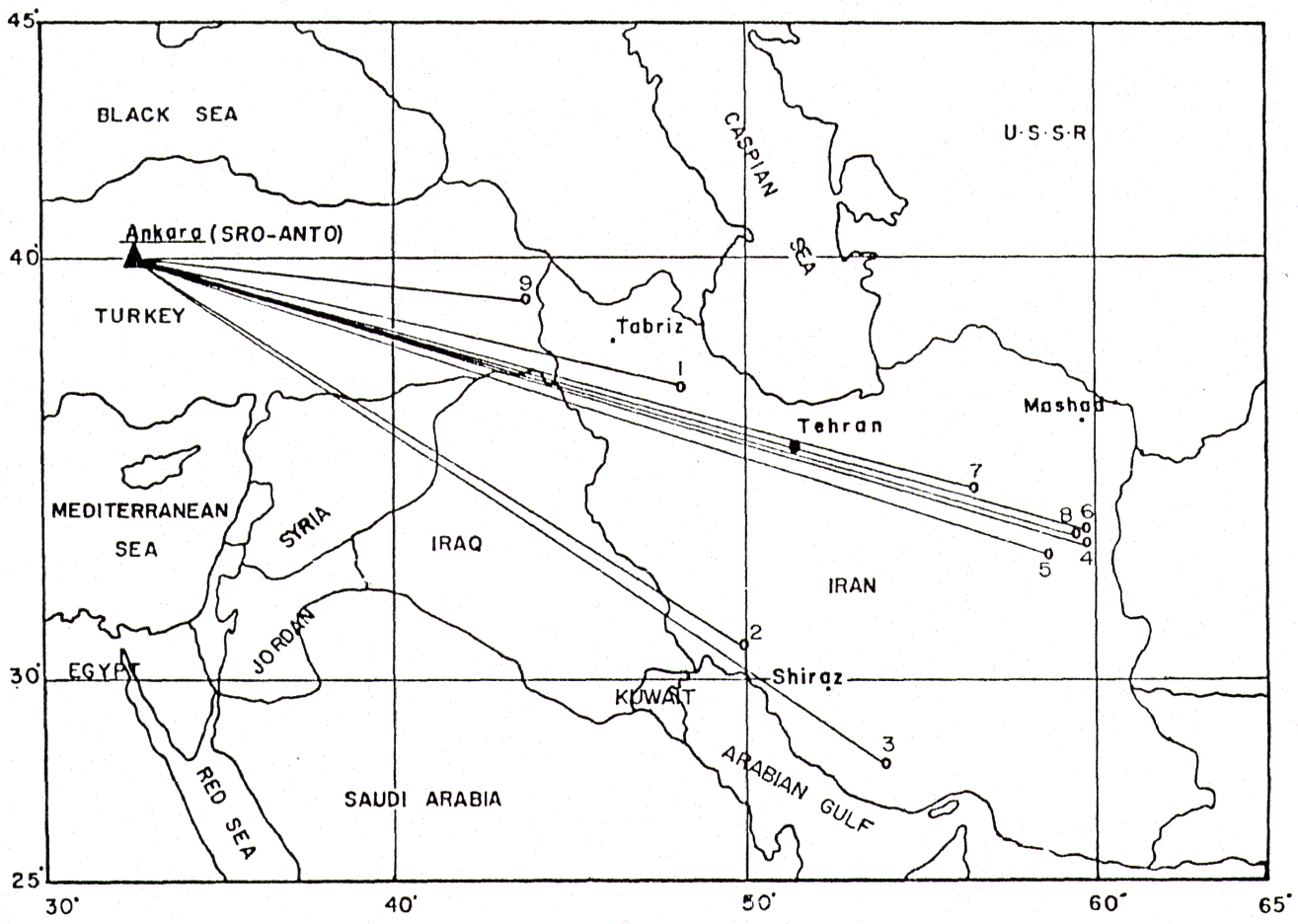

FIG. 2. Index map of epicentre locations and ray paths to ANTO.

with period. It is generally difficult to estimate the phase velocity with an accuracy corresponding to a maximum error of $\pm \pi/4$ in ϕ_0 by this technique. The reason is that for such a difference in the initial phase the discrete sets of curves are generally too close to one another.

THE DATA

The seismograms used in this work were obtained from the SRO-ANTO station. ANTO is located at the Middle East Technical University (METU), Ankara. It was set up with the cooperation of United States Geological Survey (USGS) and METU, and commenced its operations in August 1978. The output signals of 3 long period and 1 short period seismometers are recorded both analog and digital. The long period signals are sampled once per second and short period signals are sampled 20 times per second and are recorded on a magnetic tape. An event detection algorithm at the beginning of the procedure edits the short period data.

The analog records together with the Preliminary Determination of Epicentres of USGS were viewed to select well-dispersed Rayleigh waves from the earthquakes occurred in Iran and eastern Turkey. The coordinates, focal depths, origin times and magnitudes of chosen events are shown in Table I. and a location map indicating the paths is shown in Figure 2.

ANALYSES OF DATA

The analyses of seismograms were carried out in the following steps.

a -Earthquakes were chosen from PDE Monthly Listings,

b - Long period vertical seismograms of these events were viewed,

c - Well dispersed Rayleigh wave trains were selected,

d -Epicentral distances of each earthquake were computed,

e - Arrival times of each peak and trough were read from records and plotted against the peak and trough numbers,

f - Periods were found from the slope of arrival time versus peak and trough number curve,

g - Phase velocities were calculated by using equation (12),

h - Phase velocity sets were prepared for initial phases,

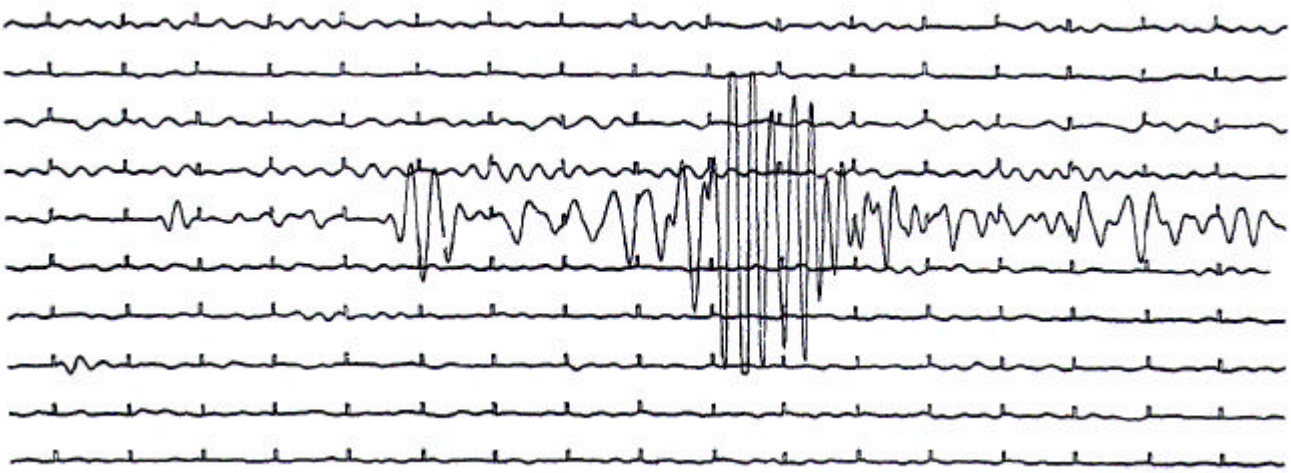

FIG. 3. A portion of ANTO LPZ seismogram of March 28, 1979 event.

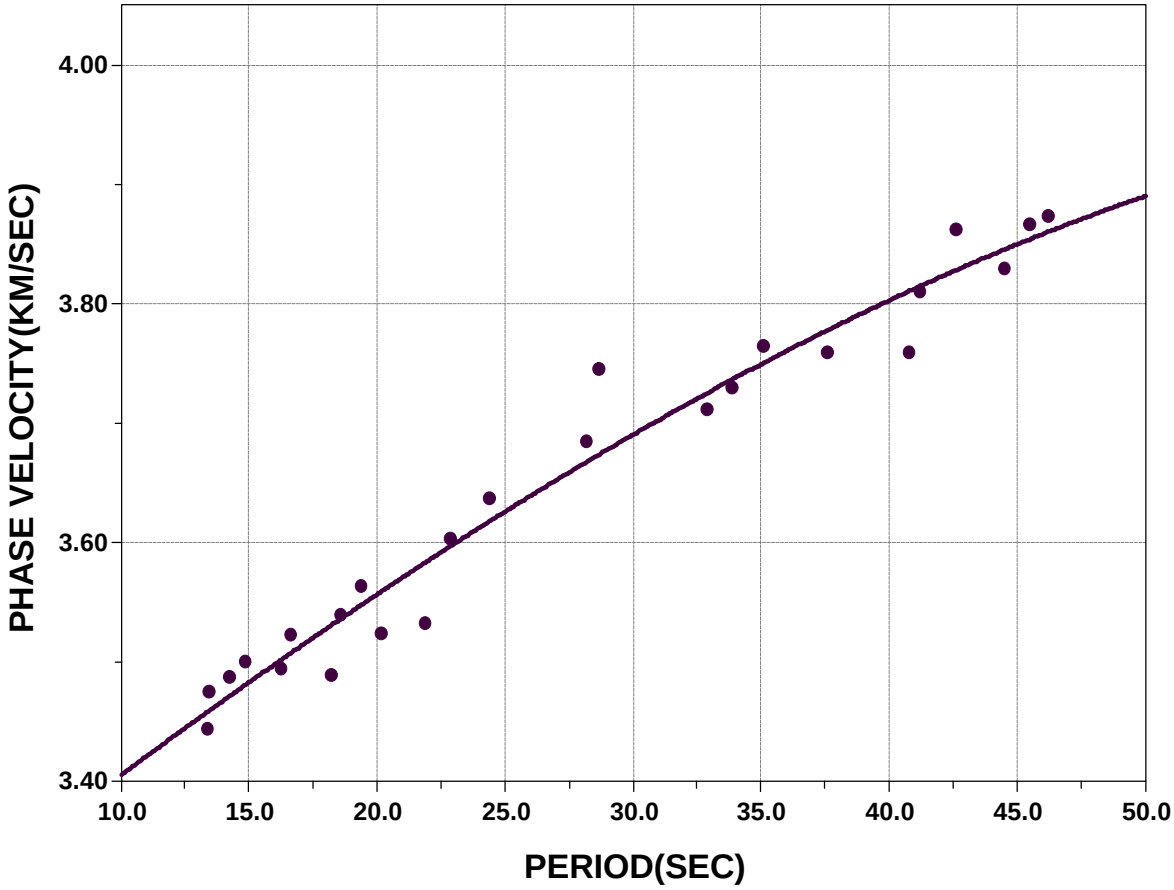

THICKNESS	P-WAVE VEL.	S-WAVE VEL.	DENSITY
3.00 KM.	5.20 KM/S	3.00 KM/S	2.55 $GMCM^{-3}$
9.00 KM.	6.10 KM/S	3.52 KM/S	2.69 $GMCM^{-3}$
19.00 KM.	6.50 KM/S	3.75 KM/S	2.85 $GMCM^{-3}$
25.00 KM.	6.80 KM/S	3.90 KM/S	3.00 $GMCM^{-3}$
	8.15 KM/S	4.70 KM/S	3.40 $GMCM^{-3}$

FIG. 4. Phase velocity versus period for eastern Iran (group I) obtained using events # 4, 5 and 6.

i - Theoretical phase velocities were calculated from the assumed earth models,

j - The observed and theoretical phase velocity curves were compared to find the best fitting theoretical curve,

k - Refinements were done by perturbing the model parameters.

l - Conclusions were drawn about the earth's structure from the assumed earth models.

Phase velocity calculations need well-dispersed wave trains. Figure 3 shows such a well-dispersed wave train on the long period seismogram of the event on March 28, 1979 in Iran as an example.

The earth may be regarded to be a vertically inhomogeneous half space and can be approximated by means of a system consisting of a large number of plane parallel homogeneous layers. The inversion may therefore be carried out most profitably where details of the layering are known. The effect of choice of active parameters on the theoretical phase velocities can be summarised as follows;

The single-layer theoretical models presented by the average values of compressional wave velocity, shear wave velocity and density give a more reliable guide to the crustal thickness. If the total thickness is fixed, the increase in number of layers gives more accurate results. Smaller density variations within the earth do not cause significant changes in velocities.

It is generally possible to find the phase velocities with an accuracy corresponding to a maximum error

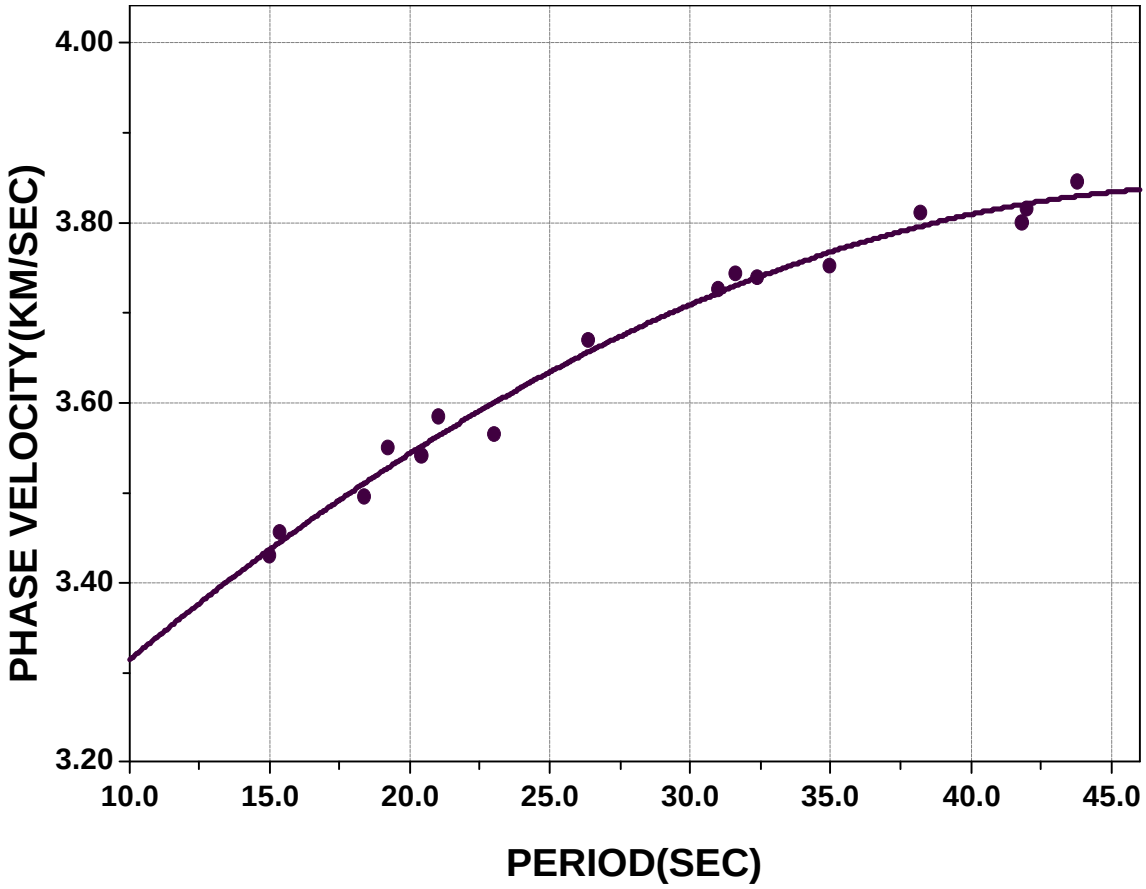

THICKNESS	P-WAVE VEL.	S-WAVE VEL.	DENSITY
3.00 KM.	5.20 KM/S	3.00 KM/S	2.55 $GMCM^{-3}$
9.00 KM.	6.10 KM/S	3.52 KM/S	2.69 $GMCM^{-3}$
17.00 KM.	6.50 KM/S	3.75 KM/S	2.85 $GMCM^{-3}$
23.00 KM.	6.80 KM/S	3.90 KM/S	3.00 $GMCM^{-3}$
	8.15 KM/S	4.70 KM/S	3.40 $GMCM^{-3}$

FIG. 5. Phase velocity versus period for eastern Iran (group II) obtained using events # 7 and 8.

of $\pm \pi/4$ in the ϕ_0 by one station method. The reason for this is that for such a difference in the initial phase, the discrete sets of curves are generally too close to one another.

But the distinction between the curves could be made better in the range of long periods (30 to 48 s) where the curves diverge.

Figure 4 shows the phase velocities computed from 3 events (events 4, 5 and 6) in eastern Iran. The set corresponding to $\phi_0 = \pi/2$ for these events gave accurate results (it was assumed that due to the closeness of epicentre locations these earthquakes started with the same initial phase). The table below the plot shows the final theoretical earth model, which yielded the best fit to the observational data.

The data for a group of 2 earthquakes (events 7 and 8) together with the theoretical curve are plotted in Figure 5, and the best fitting model parameters are shown in table below.

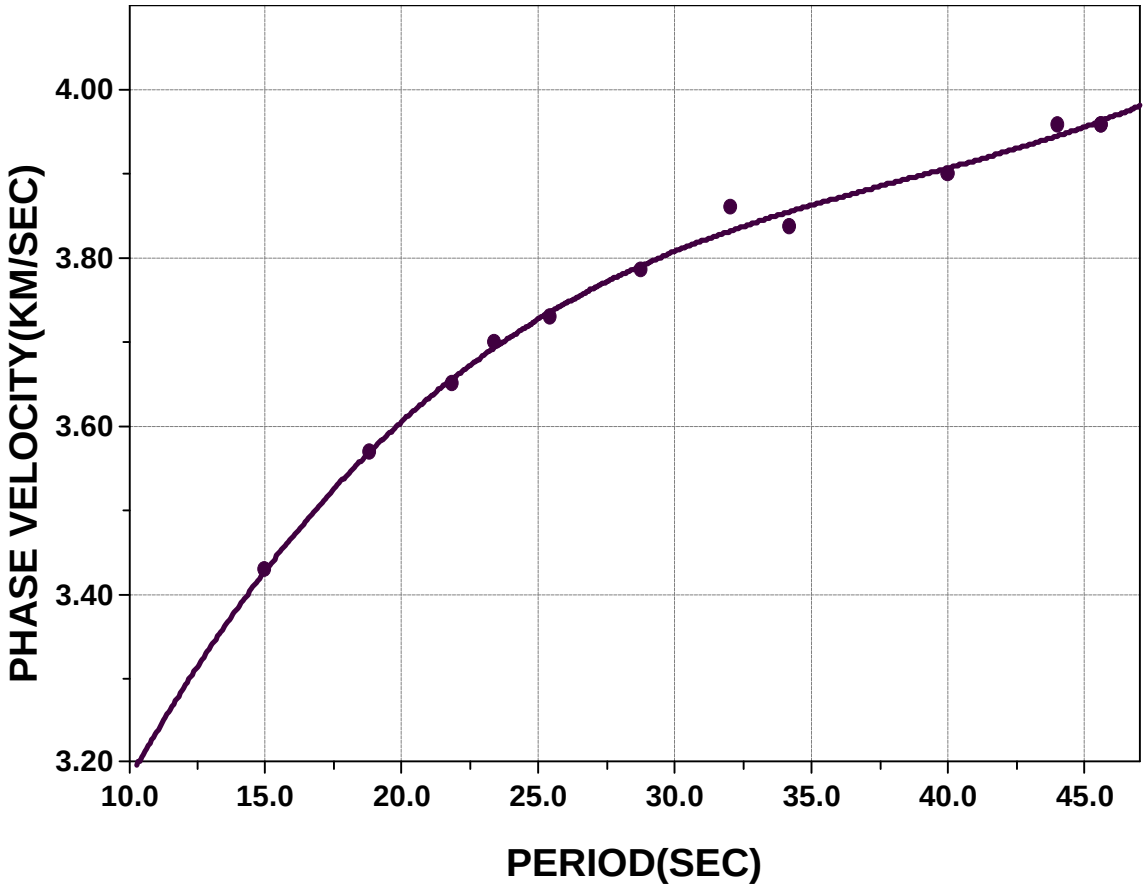

THICKNESS	P-WAVE VEL.	S-WAVE VEL.	DENSITY
5.00 KM.	5.35 KM/S	3.10 KM/S	2.60 $GMCM^{-3}$
10.00 KM.	6.10 KM/S	3.52 KM/S	2.70 $GMCM^{-3}$
13.00 KM.	6.30 KM/S	3.64 KM/S	2.85 $GMCM^{-3}$
20.00 KM.	6.70 KM/S	3.87 KM/S	3.00 $GMCM^{-3}$
	8.15 KM/S	4.70 KM/S	3.40 $GMCM^{-3}$

FIG. 6. Phase velocity versus period for southwestern Iran (group I) obtained using events 2 and 3 (initial phase $\pi/2$).

In Figures 6 and 7 the data along 2 paths from southwestern Iran (events 2 and 3) to ANTO are illustrated. Initial phases were assumed to be $\pi/2$ and $\pi/4$, respectively. The tables below these plots list the conclusive models.

The data from one earthquake in northwestern Iran (event 1) and for one earthquake (event 9) in eastern. Turkey are shown in Figures 8 and 9 together with the best fitting models. The possible initial phases were 0 and $\pi/2$, respectively.

The resulting velocities are almost equal to continental type of velocities. The first layer is interpreted as to be made of consolidated sedimentary rocks (velocity of P waves are between 5.0 km/s and 5.35 km/s). The velocity of 6.1 km/s represents a fractured granitical layer. Underlying layer is unfractured granitic layer with P wave velocities ranging from 6.3 to 6.5 km/s. These two granitic layers represent the upper crust, whereas the lowest layer represents the lower crust. The last velocity represents the upper mantle.

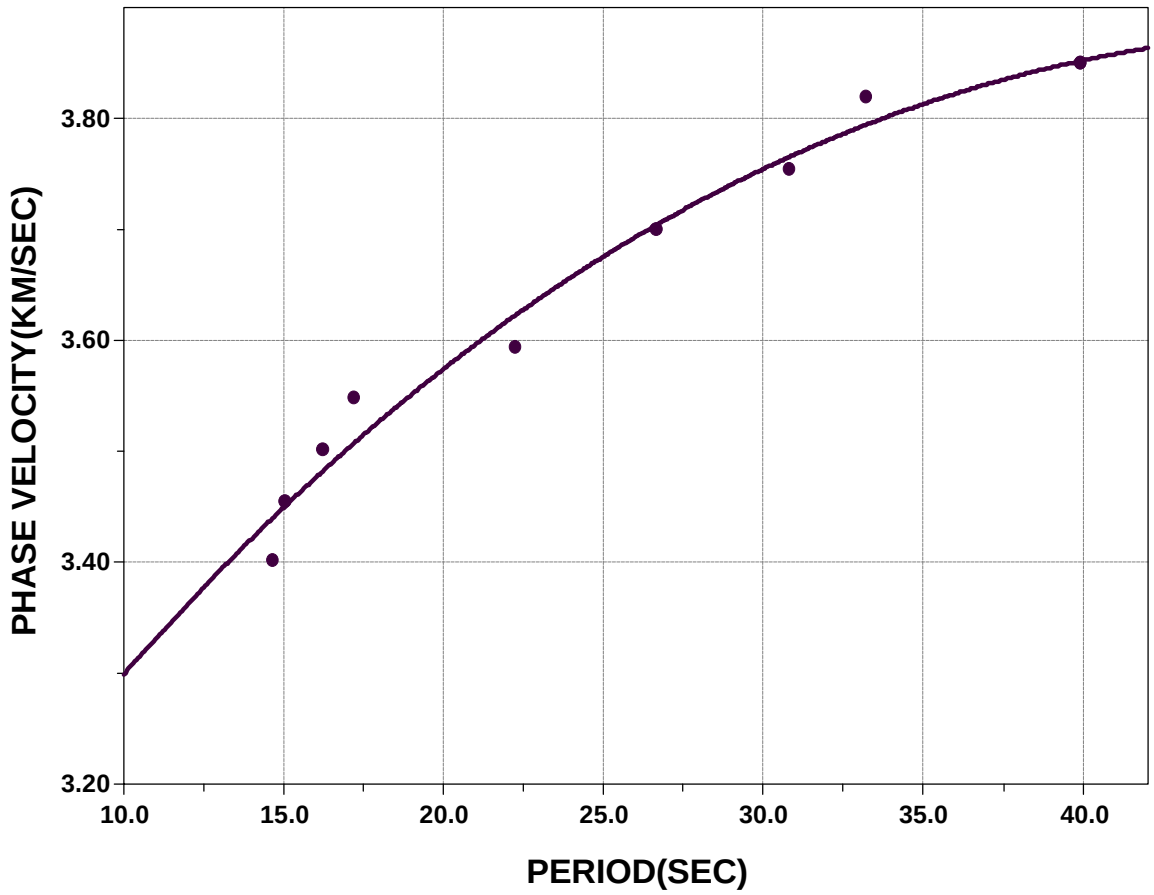

THICKNESS	P-WAVE VEL.	S-WAVE VEL.	DENSITY
4.00 KM.	5.35 KM/S	3.10 KM/S	2.60 $GMCM^{-3}$
9.00 KM.	6.10 KM/S	3.52 KM/S	2.70 $GMCM^{-3}$
13.00 KM.	6.30 KM/S	3.64 KM/S	2.85 $GMCM^{-3}$
19.00 KM.	6.70 KM/S	3.87 KM/S	3.00 $GMCM^{-3}$
	8.15 KM/S	4.70 KM/S	3.40 $GMCM^{-3}$

FIG. 7. Phase velocity versus period for southwestern Iran(group II) obtained using events # 2 and 3 (initial phase $\pi/4$).

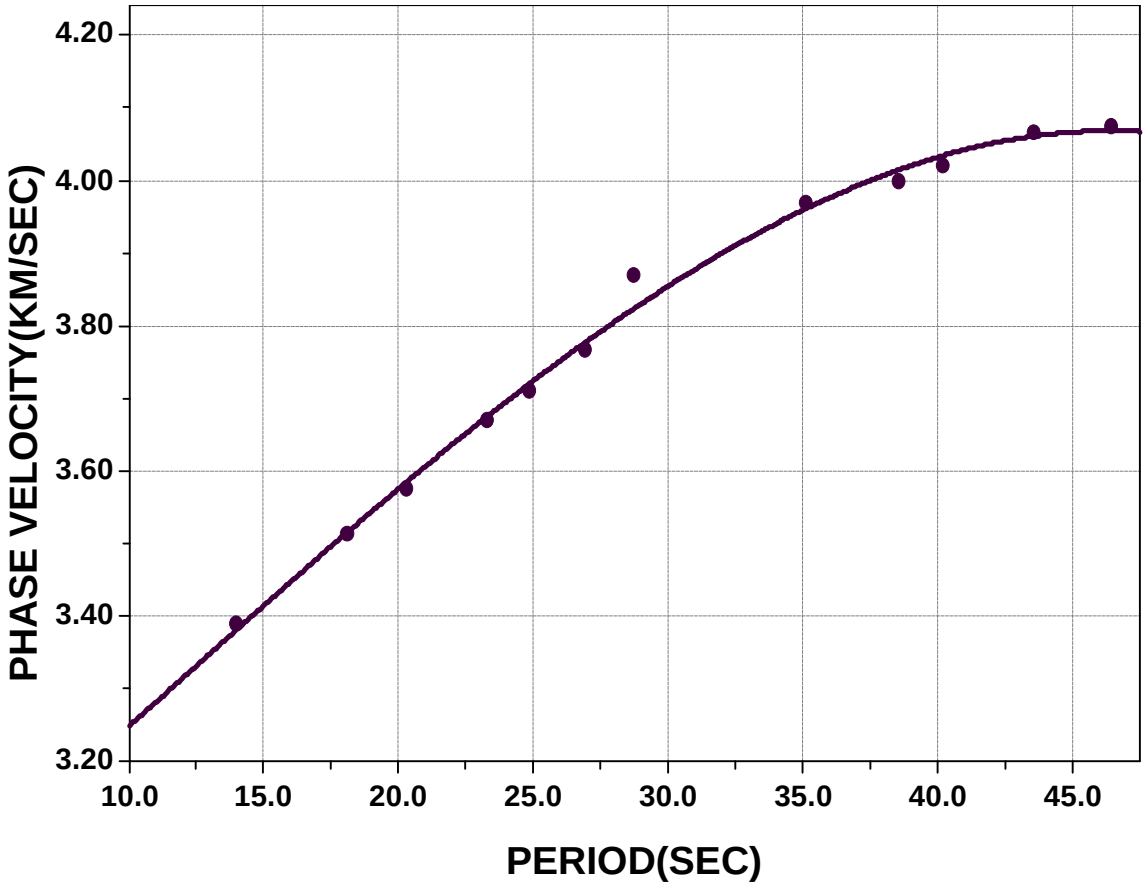

THICKNESS	P-WAVE VEL.	S-WAVE VEL.	DENSITY
3.00 KM.	5.20 KM/S	3.00 KM/S	2.55 GMCM^{-3}
9.00 KM.	6.10 KM/S	3.52 KM/S	2.70 GMCM^{-3}
15.00 KM.	6.30 KM/S	3.64 KM/S	2.85 GMCM^{-3}
17.00 KM.	6.70 KM/S	3.87 KM/S	3.00 GMCM^{-3}
	8.15 KM/S	4.70 KM/S	3.40 GMCM^{-3}

FIG. 8. Phase velocity versus period for northwestern Iran using event # 1 (initial phase 0).

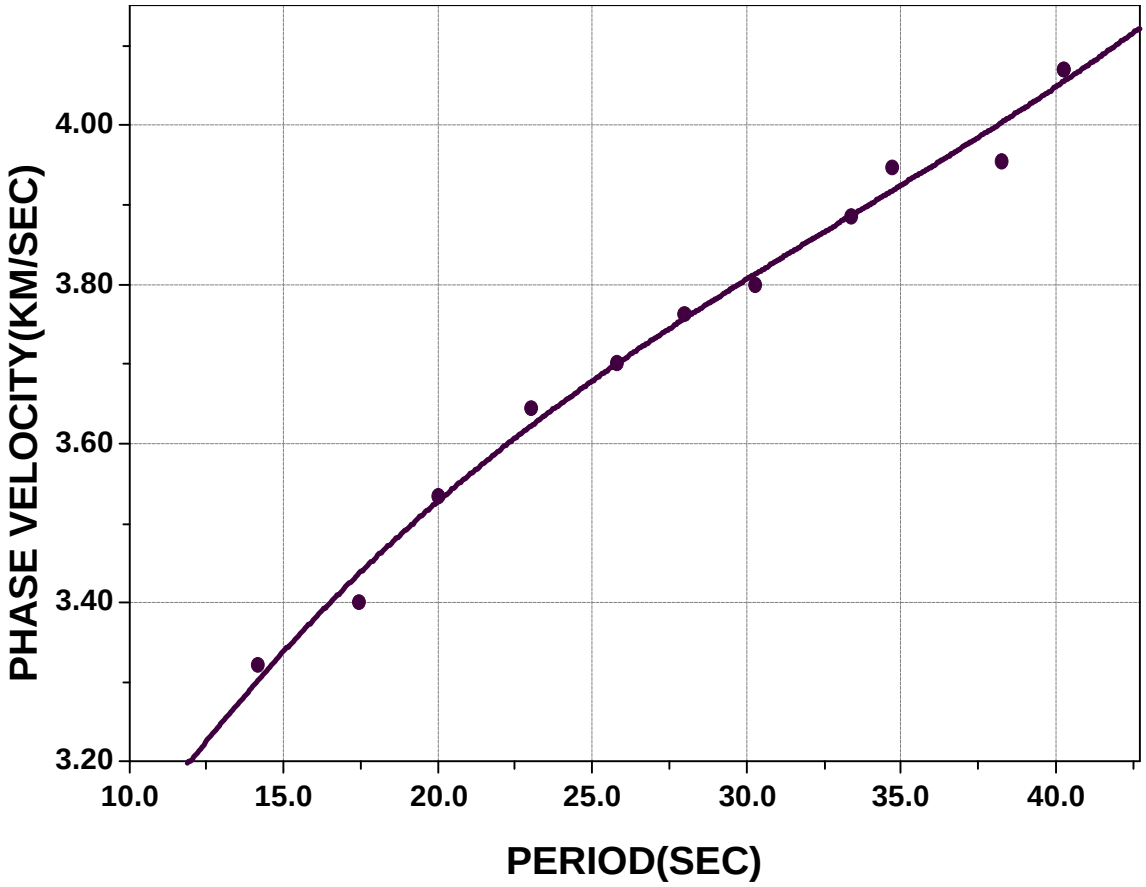

THICKNESS	P-WAVE VEL.	S-WAVE VEL.	DENSITY
2.00 KM	5.20 KM/S	3.00 KM/S	2.55 GMCM^{-3}
9.00 KM	6.10 KM/S	3.52 KM/S	2.70 GMCM^{-3}
15.00 KM	6.30 KM/S	3.64 KM/S	2.85 GMCM^{-3}
16.00 KM	6.70 KM/S	3.87 KM/S	3.00 GMCM^{-3}
	8.15 KM/S	4.70 KM/S	3.40 GMCM^{-3}

FIG. 9. Phase velocity versus period for eastern Turkey obtained using event # 9 (initial phase $\pi/2$).

CONCLUSIONS

Observed Rayleigh wave phase velocities in the period range between 12 and 48 seconds for eastern Turkey and Iran were calculated. The theoretical dispersion curves were computed for an initial model. The observational curves were tried to match with theoretical ones. The model parameters were perturbed and dispersion curves were recalculated until the best fit was obtained. The final models and observed phase velocity plots are shown in Figures 4 to 9.

The data along the path between east of Iran and ANTO fit to a model with a total crustal thickness 52 to 56 km. This thickness decrease downs to 45-48 km along the path between southwestern of Iran and ANTO and to 42-44 km along the path between eastern Turkey- northeastern of Iran to ANTO.

The method gives good results if the phase velocity is known at least at one period by some other method. For example, if observations for very long periods are included in the data one may use the fact that the phase velocities for very long periods are generally the same for continental and oceanic structure and are known with sufficient accuracy.

REFERENCES

Akaschek, B. and Nassari, S., 1972, Dis Machtigkeit der Erdkruste in Iran: Journal of the Earth and Space Physics, **1**, 1-6.

Asudeh, I., 1982a, P_n velocities beneath Iran: Earth and Planetary Science Letters, **61**, 136 - 142.

Asudeh, I., 1982b, Seismic structure of Iran from surface and body wave data: Geophysical Journal of R.A.S., **71**, 715 - 730.

Brune, N. J., Nafe J. E. and Oliver, J.E., 1960, A simplified method for the analyses and synthesis of dispersed wave trains: Journal of Geophysical Research, **65**, 287-303.

Canitez, N. and Ezen U., 1975, Ardisik filitre teknigi ile Asya, Avrupa ve Afrika'da yuzey dalgalarinin incelenmesi (in Turkish): Istanbul Teknik Universitesi, Maden Fakültesi.

Chen, C. Y., Chen, W. P. and Molnar, P., 1980, The uppermost mantle P wave velocities beneath Turkey and Iran: Geophysical Research Letters, **7**, 77-80.

Eslami, A. A.1974, Detecting the thickness of the crust in Shiraz area using hypocenter situated below the crust: Journal of the Earth and Space Physics, **2**, 15-18

Herrmann, R. B., 1978, Computer programs in earthquake seismology: St.Louis University, Missouri.

Necioglu, A., Maddison B. and Turkelli, N., 1981, A study of crustal and upper mantle structure of northwestern Turkey: Geophysical Research Letters, **8**, 33-35.

Sneyder D. B. M. and Barazangi, M., 1986, Deep crustal structure and flexure of the Arabian plate beneath the Zagros collisional mountain belt as inferred from gravity observations: Tectonics, **5**, 361-373.

Spencer, E. W., 1977, Introduction to the Structure of the Earth: McGraw-Hill Kogakushha Ltd, Tokyo.